Interaction between the N- and C-Terminal Domains Modulates the Stability and Lipid Binding of Apolipoprotein A-I[†]

Mao Koyama,[‡] Masafumi Tanaka,[‡] Padmaja Dhanasekaran,[§] Sissel Lund-Katz,[§] Michael C. Phillips,[§] and Hiroyuki Saito*[,‡]

Department of Biophysical Chemistry, Kobe Pharmaceutical University, 4-19-1 Motoyamakitamachi, Higashinada-ku, Kobe 658-8558, Japan, and Division of GI/Nutrition/Hepatology, The Children's Hospital of Philadelphia, University of Pennsylvania School of Medicine, Philadelphia, Pennsylvania 19104-4318

Received December 18, 2008; Revised Manuscript Received January 13, 2009

ABSTRACT: The tertiary structures of human and mouse apolipoprotein A-I (apoA-I) are comprised of an N-terminal helix bundle and a separate C-terminal domain. To define the possible intramolecular interaction between the N- and the C-terminal domains, we examined the effects on protein stability and lipid-binding properties of exchanging either the C-terminal domain or helix between human and mouse apoA-I. Chemical denaturation experiments demonstrated that replacement of the C-terminal domain or helical segment in human apoA-I with the mouse counterparts largely destabilizes the N-terminal helix bundle. Removal of the C-terminal domain or α-helix in human apoA-I had a similar effect on the destabilization of the helix bundle against urea denaturation, indicating that the C-terminal helical segment mainly contributes to stabilizing the N-terminal helix bundle structure in the apoA-I molecule. Consistent with this, KI quenching experiments indicated that removal or replacement of the C-terminal domain or helix in human apoA-I causes Trp residues in the N-terminal domain to become exposed to solvent. Measurements of the heats of binding to egg phosphatidylcholine (PC) vesicles and the kinetics of solubilization of dimyristoyl PC vesicles demonstrated that the destabilized human N-terminal helix bundle can strongly interact with lipids without the hydrophobic C-terminal helix. In addition, site-specific labeling of the N- and C-terminal helices by acrylodan to probe the conformational stability and the spatial proximity of the two domains indicated that the C-terminal helix is located near the N-terminal helix bundle, leading to a relatively less solvent-exposed, more organized conformation of the C-terminal domain. Taken together, these results suggest that interaction between the N- and C-terminal tertiary structure domains in apoA-I modulates the stability and lipid-binding properties of the N-terminal helix bundle.

Apolipoprotein A-I (apoA-I[1]) is the major protein of plasma high density lipoprotein (HDL) and functions as a critical mediator in reverse cholesterol transport, a process by which excess cholesterol in peripheral cells is transferred via HDL to the liver for catabolism (*1*−*3*). Although apoA-I exists primarily in a lipid-bound state on HDL particles in plasma, lipid-free apoA-I is known to be a physiologically relevant acceptor of cell-derived cholesterol via adenosine 5′-triphosphate (ATP) binding cassette transporter A1 (ABCA1) (*4, 5*). The interaction of lipid-free apoA-I with functional ABCA1 results in the lipidation of apoA-I and formation of nascent HDL particles, in which a multistep mechanism seems to be involved with this reaction process (*6*−*8*).

Human apoA-I is a 243-residue polypeptide that contains characteristic 11- and 22-residue repeats of amphipathic α-helices (*9*). The N- and C-terminal helical regions in the apoA-I molecule contribute to the strong lipid-binding properties of this protein (*10*−*12*) as well as its conformational stability in solution (*13, 14*). It has been demonstrated recently that the apoA-I molecule folds into two tertiary structure domains, comprising an N-terminal α-helix bundle spanning residues 1−187 and a separate, less organized C-terminal region spanning the remainder of the molecule (*15*−*17*). Since mouse apoA-I, which has 65% amino acid identity to human apoA-I, also adopts a similar two-domain structure (*18*), the ability to fold into two domains seems to be a general feature of the apoA-I molecule regardless of the species of origin. However, the links between the two-domain structure and the function of apoA-I remain to be established (*19*). For example, it is not known why the lipid binding properties of human and mouse apoA-I are different in that they form HDL particles of different sizes; the mouse protein forms a single population of larger HDL particles whereas human apoA-I forms two subpopulations, HDL_2 and HDL_3 (*20, 21*).

* To whom correspondence should be addressed. E-mail: saito@kobepharma-u.ac.jp. Tel: +81-78-441-7539. Fax: +81-78-441-7541.

[†] This work was supported by NIH grant HL22633, Grant-in-Aid for Scientific Research from JSPS, and Takeda Science Foundation.

[‡] Kobe Pharmaceutical University.

[§] University of Pennsylvania School of Medicine.

[1] Abbreviations: ABCA1, ATP-binding cassette transporter A1; ANS, 8-anilino-1-naphthalenesulfonic acid; Ac, acrylodan; apoA-I, apolipoprotein A-I; CD, circular dichroism; DMPC, dimyristoylphosphatidylcholine; FRET, fluorescence resonance energy transfer; GP, generalized polarization; GdnHCl, guanidine hydrochloride; HDL, high density lipoprotein; ITC, isothermal titration calorimetry; PC, phosphatidylcholine; SUV, small unilamellar vesicle; WMF, wavelength of maximum fluorescence; WT, wild type.

10.1021/bi802317v CCC: $40.75
Published on Web 02/24/2009

Although the X-ray crystal structure of the lipid-free apoA-I clearly demonstrates the compactly folded, highly ordered two-domain structure (*17*), it appears that the true conformation in solution is more flexible and less organized than the conformation in its crystal state (*22, 23*). The α-helix content of approximately 82% found in the crystal structure is much higher than the approximately 50% found for monomeric apoA-I in solution (*11, 24*). Indeed, a recent electron paramagnetic resonance spectroscopy study showed that the N-terminal region (residues 1−98) is heterogeneous in its secondary structure, including a short segment of β-strand structure (*25*). Interestingly, this β-strand structure is similar in length to the β-strand observed in the C-terminus (*26*), suggesting the potential of these regions to participate in intra- or interdomain interaction.

It has been proposed that the interactions between the N- and the C-terminal segments in apoA-I are involved in maintaining the stability of the lipid-free conformation (*13, 14, 16, 27*). Fluorescence resonance energy transfer (FRET) studies demonstrated that the C-terminal residues 190 and 232 are in close proximity to the four Trp residues in the N-terminal domain of apoA-I (*28, 29*). In agreement with this, the homology modeling based on cross-link distance constraints predicts that the N- and C-termini of lipid-free apoA-I are situated in relatively close proximity (*16*). Such interactions between the N- and C-terminal segments also seem to modulate the lipid-binding ability and ABCA1-mediated cholesterol efflux by apoA-I (*14, 30−32*). However, the detailed molecular nature of the N- and C-terminal interaction in apoA-I is unknown to date.

Here, we examined the effects of truncation or substitution of the C-terminal domain or helical segment on the protein stability and lipid-binding properties to define the intramolecular interaction between the N- and the C-terminal domains in apoA-I. In addition, we used site-specific fluorescence labeling of the N- and C-terminal helices to probe the conformational stability and the spatial proximity of the two domains. The results suggest that the C-terminal helix is located near the N-terminal helix bundle, modulating the conformational stability and lipid-binding properties of apoA-I.

EXPERIMENTAL PROCEDURES

Proteins and Peptide. Human/mouse apoA-I hybrid molecules were engineered using the Stratagene (La Jolla, CA) domain-swap protocol (*18*). The mutations in human apoA-I to introduce cysteine residue into Val-53 or Phe-229 were made using the QuikChange site-directed mutagenesis kit (Stratagene). Human and mouse wild type (WT) apoA-I and engineered mutants were expressed and purified as described (*15, 18*). The apoA-I preparations were at least 95% pure as assessed by sodium dodecyl sulfate polyacrylamide gel electrophoresis. The C-terminal apoA-I 220−241/F229C peptide was synthesized at Sigma Genosys (Hokkaido, Japan) with an acetylated N-terminus and an amidated C-terminus. Peptide purity was verified by analytical high-performance liquid chromatography (>97%) and mass spectrometry. In all experiments, apoA-I variants and peptide were freshly dialyzed from 6 M guanidine hydrochloride (GdnHCl) solution (+1% β-mercaptoethanol for the cysteine-containing mutants) into the appropriate buffer before use.

Site-Specific Acrylodan (Ac) Labeling. Cysteine-containing apoA-I variants or peptide were incubated with 10-fold molar excess of tris(2-carboxyethyl)phosphine hydrochloride (Pierce, Rockford, IL) for 1 h to reduce the sulfhydryl group. The 10 mM stock solution of 6-acryloyl-2-dimethylaminonaphthalene (acrylodan; Molecular Probes, Inc., Eugene, OR) in dimethylformamide was added so that a final molar ratio of probe to protein was 10:1 (or 3:1 for peptide). The reaction mixtures were then stirred at room temperature for 3 h in the dark. Unreacted acrylodan was removed by extensive dialysis at 4 °C in Tris buffer (10 mM Tris, 150 mM NaCl, 1 mM EDTA, 0.02% NaN_3, pH 7.4). The degree of labeling was determined using the extinction coefficient for acrylodan of 19 200 M^{-1} cm^{-1} at 391 nm and found to be over 90%.

Preparation of Small Unilamellar Vesicles (SUVs). SUVs were prepared as described (*11, 14*). Briefly, a film of egg phosphatidylcholine (PC) on the wall of a glass tube was dried under vacuum overnight. The lipid was then hydrated in Tris buffer and sonicated on ice under nitrogen. After removing titanium debris, the samples were centrifuged in a Beckman TLA110 rotor for 2 h at 4 °C at 51 000 rpm to separate any remaining large vesicles. The PC concentration of SUV was determined using an enzymatic assay kit from Wako Pure Chemicals (Osaka, Japan).

Circular Dichroism (CD) Spectroscopy. Far-UV CD spectra were recorded from 185 to 260 nm at 25 °C using an Aviv 62DS spectropolarimeter. After dialysis from 6 M GdnHCl solution, the apoA-I sample was diluted to 25−50 μg/mL in 10 mM sodium phosphate buffer (pH 7.4), and the CD spectrum was obtained. The results were corrected by subtracting the buffer baseline. The α-helix content was calculated from the molar ellipticity at 222 nm, as described (*33*). For monitoring chemical denaturation, proteins at a concentration of 50 μg/mL were incubated overnight at 4 °C with GdnHCl or urea at various concentrations. K_D at a given denaturant concentration was calculated from the ellipticity values, and the free energy of denaturation, $\Delta G_D°$, the midpoint of denaturation, $D_{1/2}$, and the m value which reflects the cooperativity of denaturation in the transition region were determined by the linear equation $\Delta G_D = \Delta G_D° - m$[denaturant], where $\Delta G_D = -RT \ln K_D$ (*14, 33*).

Fluorescence Measurements. Fluorescence measurements were carried out with a Hitachi F-7000 fluorescence spectrophotometer at 25 °C in Tris buffer (pH 7.4). Trp emission fluorescence of proteins at a concentration of 25 μg/mL was recorded from 300 to 420 nm using a 295 nm excitation wavelength to avoid tyrosine fluorescence. Acrylodan emission fluorescence of proteins or peptide (5−25 μg/mL) was collected from 380 to 600 nm using a 360 nm excitation wavelength. For chemical denaturation experiments, $\Delta G_D°$, $D_{1/2}$, and the m value were determined by monitoring the change in wavelength of maximum fluorescence (WMF) of intrinsic Trp residues (*15*) or the generalized polarization (GP) of acrylodan (*34*). The GP value is given by $GP = (I_B - I_R)/(I_B + I_R)$, where I_B and I_R are the emission intensities at the blue (450 or 460 nm) and red (520 nm) edges of the emission spectrum, respectively. In fluorescence quenching experiments, the Trp or acrylodan emission spectra of proteins were recorded at increasing concentrations of KI (0−0.56 M) using a 5 M stock solution containing 1 mM NaS_2O_3 to prevent the formation of iodine. After correction for dilution, the integrated fluorescence intensities were

Table 1: α-Helix Content and Parameters for Urea Denaturation of apoA-I Variants Monitored by Molar Ellipticity or Trp Fluorescence

		molar ellipticity			Trp fluorescence		
apoA-I variant	α-helix (%)	$\Delta G_D°$, kcal/mol	m	$D_{1/2}$, M	$\Delta G_D°$, kcal/mol	m	$D_{1/2}$, M
human WT	46 ± 3	3.6 ± 0.1	1.33 ± 0.04	2.7 ± 0.2	6.2 ± 0.2	2.0 ± 0.1	3.0 ± 0.2
h(1−189)/m(187−240)	45 ± 2	1.6 ± 0.1[b]	0.67 ± 0.03[b]	2.4 ± 0.2	3.1 ± 0.1[b]	1.3 ± 0.1[b]	2.5 ± 0.1[b]
h(1−220)/m(218−240)	47 ± 2	1.8 ± 0.1[b]	0.78 ± 0.04[b]	2.3 ± 0.2[a]	3.3 ± 0.2[b]	1.3 ± 0.1[b]	2.5 ± 0.2[a]

[a] $P < 0.05$. [b] $P < 0.01$ compared to WT apoA-I.

plotted according to the Stern-Volmer equation, $F_0/F = 1 + K_{sv}[KI]$, where F_0 and F are the fluorescence intensities in the absence and presence of quencher, respectively, and K_{sv} is the Stern-Volmer constant. Quenching parameters were obtained by fitting to the modified Stern-Volmer equation, $F_0/(F_0 - F) = 1/f_a + 1/f_aK_{sv}[KI]$, where f_a is the fraction of Trp residues accessible to the quencher. Steady-state fluorescence anisotropy of acrylodan was measured with an excitation at 360 nm and an emission at 485 nm, as described (*35*). 8-Anilino-1-naphthalenesulfonic acid (ANS) fluorescence spectra were collected from 400 to 600 nm at an excitation wavelength of 395 nm in the presence of 50 μg/mL protein and an excess of ANS (250 μM) (*15*).

For FRET experiments, the emission spectra of acrylodan-labeled and unlabeled apoA-I variants were measured from 300 to 600 nm with an excitation of 295 nm. FRET efficiency (E) was calculated according to $E = 1 - F_{DA}/F_D$, where F_{DA} is the fluorescence intensity of the donor with acrylodan attached and F_D is the fluorescence intensity of the donor lacking acrylodan. The FRET distance (R) was calculated according to $E = R_0^6/(R_0^6 + R^6)$, where R_0 is the Förster radius for energy transfer from Trp to acylodan in a protein (2.7 nm) (*36*).

DMPC Clearance Assay. The kinetics of solubilization of DMPC multilamellar vesicles by the apoA-I variants were measured by monitoring the time-dependent decrease in turbidity (*18, 37*). DMPC vesicles extruded through a 200 nm filter were mixed with apoA-I samples to a final volume of 600 μL in a cuvette and incubated for 15 min at 24.6 °C. Sample light scattering intensity was monitored at 325 nm on a Shimadzu UV-2450 spectrophotometer and normalized the initial scattering intensity value to 1.

Isothermal Titration Calorimetry (ITC) Measurements. Heats of apoA-I binding to SUV were measured with a MicroCal MCS isothermal titration calorimeter at 25 °C (*11, 38*). To measure the enthalpy of binding at a low surface concentration, apoA-I solutions were injected into SUV in the cell at a PC-to-protein molar ratio of >10 000 where the injected protein binds completely to the SUV surface. The heat of dilution was determined in the control experiment by injecting apoA-I solution into buffer and was subtracted from the heat determined in the corresponding apoA-I−SUV binding experiments.

RESULTS

Urea Denaturation of Human/Mouse apoA-I Hybrid Molecules. The primary structures of human and mouse apoA-I are 65% identical, with the N- and C-terminal domains being 70% and 46% identical, respectively (*39*). We have demonstrated previously that both proteins adopt a similar two-domain tertiary structure, comprising an N-terminal helix bundle domain and a separate C-terminal domain (*18*). Interestingly, exchanging the C-terminal domains between human and mouse apoA-I to create human−mouse hybrid molecules affected the stability of the N-terminal helix bundle against GdnHCl, suggesting an energetic contribution of interactions between the N- and C-terminal domains to the overall stability of apoA-I (*18*). To follow up this possible interaction between the N- and C-terminal domains in apoA-I, we examined the effects of exchanging the C-terminal domain or α-helix between human and mouse apoA-I on the protein stability against urea denaturation. The electrostatic interactions between amino acids are shielded by GdnHCl, whereas uncharged urea has no effect on the electrostatic interactions (*40*). Thus, we can estimate the contribution of the electrostatic interactions to the protein stability by comparing denaturation behaviors in both denaturants.

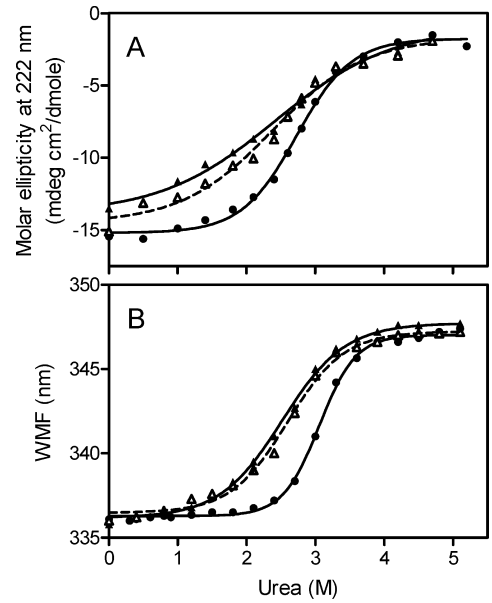

FIGURE 1: Urea-induced denaturation of human and mouse hybrid apoA-I monitored by molar ellipticity (A) or Trp fluorescence (B): ● = human WT, ▲ = apoA-I h(1−189)/m(187−240), △ = apoA-I h(1−220)/m(218−240). Protein concentration was 50 μg/mL.

As shown in Table 1, replacement of the C-terminal domain or α-helix in human apoA-I with the mouse counterparts to create the human(h)/mouse(m) hybrid apoA-I molecules h(1−189)/m(187−240) and h(1−220)/m(218−240) results in no change in α-helix content (*18*). However, both apoA-I hybrid molecules exhibited greatly decreased stability against urea denaturation compared to human WT apoA-I as monitored by molar ellipticity (Figure 1A) and Trp fluorescence (Figure 1B). Comparison of the thermodynamic parameters such as the free energy and midpoint of denaturation between apoA-I h(1−189)/m(187−240) and h(1−220)/m(218−240) revealed that the substitutions of the C-terminal domain or α-helix in human apoA-I by the mouse counterparts have similar destabilizing effects on the protein (Table 1). It should be noted

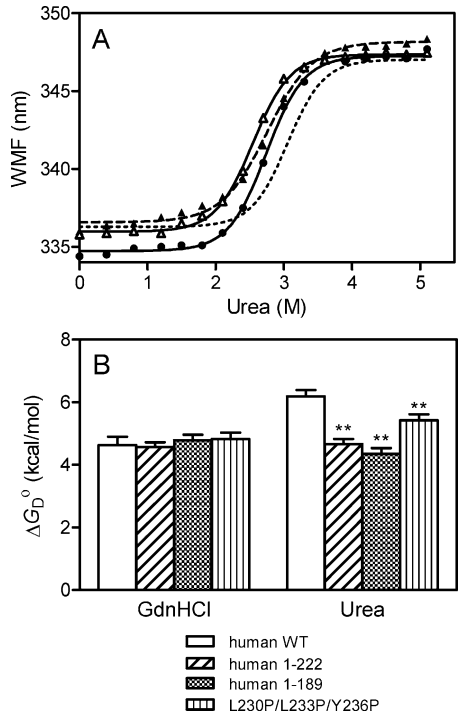

FIGURE 2: Chemical denaturation of the C-terminal truncated human apoA-I mutants monitored by Trp fluorescence. (A) Urea-induced denaturations of human WT (dotted line), human 1−222 (△), human 1−189 (▲), and human L230P/L233P/Y236P (●) are plotted. Protein concentration was 25 μg/mL. (B) Comparison of the free energies of denaturation induced by GdnHCl and urea is shown. $^{**}P < 0.01$ is compared to human WT apoA-I (ΔG_D° in GdnHCl and urea denaturation are 4.6 ± 0.3 and 6.2 ± 0.2 kcal/mol, respectively).

that since all Trp residues are located in the N-terminal helix bundle domain (positions 8, 50, 72, and 108), Trp fluorescence reflects the conformational change of the N-terminal helix bundle. Thus, it follows that the substitution of the human C-terminal α-helix with the equivalent mouse C-terminal segment mainly contributes to the destabilization of the human N-terminal helix bundle by the mouse C-terminal domain. In addition, large differences in ΔG_D° and *m* values monitored by molar ellipticity and Trp fluorescence such as 3.6 versus 6.2 kcal/mol for ΔG_D° of human WT (Table 1) appear to come from the fact that molar ellipticity measures only unfolding of α-helical structure, whereas Trp fluorescence measures unfolding of tertiary structure as well so that disruption of helix−helix contacts is included in the free energy change (*41*).

Effects of Removal or Disruption of the C-Terminal Helix on Chemical Denaturation of Human apoA-I. To further examine the contribution of the C-terminal α-helix to the stability of the N-terminal helix bundle in human apoA-I, we used the C-terminally truncated mutants apoA-I 1−222 and 1−189 (*15*) or proline-inserted mutant apoA-I L230P/L223P/Y236P, in which the C-terminal α-helical structure is disrupted (*14, 42*). Previous studies showed that such removal or disruption of the C-terminal α-helix in apoA-I has no effect on the stability of the N-terminal helix bundle against GdnHCl denaturation (*14, 15*). In contrast, these mutations in the C-terminal α-helix destabilized the N-terminal helix bundle against urea denaturation as monitored by Trp fluorescence (Figure 2A). Comparison of the free energies of denaturation by GdnHCl and urea (Figure 2B) clearly demonstrates that the C-terminal α-helix stabilizes the N-terminal helix bundle of apoA-I against urea denaturation but not against GdnHCl denaturation. This suggests the possible involvement of electrostatic interactions in the stabilization of the N-terminal helix bundle by the C-terminal α-helix. Similar destabilization of the C-terminally truncated mutants against urea denaturation was also observed by monitoring the molar ellipticity (data not shown).

Table 2: Parameters of KI Quenching of Trp Fluorescence and ANS Binding of apoA-I Variants

	KI quenching		
apoA-I variant	f_a	K_{SV}, M^{-1}	ANS fluorescence[a]
human WT	0.67 ± 0.03	4.7 ± 0.3	1.0
human 1−189	0.67 ± 0.02	6.0 ± 0.2[c]	0.6
human 1−222	0.64 ± 0.02	5.7 ± 0.2[c]	0.6
h(1−189)/m(187−240)	0.65 ± 0.02	5.7 ± 0.3[c]	0.8
h(1−220)/m(218−240)	0.67 ± 0.02	5.2 ± 0.2[b]	0.8

[a] Values are relative to WT. Estimated error is within ± 0.1. [b] $P < 0.05$. [c] $P < 0.01$ compared to WT apoA-I.

KI Quenching and ANS Binding of Human apoA-I C-Terminal Mutants. We next performed KI quenching of Trp fluorescence and ANS binding experiments for the apoA-I variants to monitor the tertiary structural change induced by the C-terminal truncation or substitution. As shown in Table 2, significant increases in K_{SV} values for the C-terminally truncated or substituted mutants were observed compared to WT apoA-I, indicating that Trp residues in these C-terminal mutants are more exposed to the aqueous phase. ANS fluorescence results indicate that there is decreased hydrophobic surface exposure in the C-terminal mutants because of removal or replacement of the hydrophobic human C-terminal domain or α-helix with the more polar and disordered mouse counterparts (*18*).

Lipid-Binding Properties of Human/Mouse apoA-I Hybrid Molecules. To assess the lipid-binding properties of the human−mouse hybrid apoA-I, we compared their abilities to solubilize DMPC vesicles (DMPC clearance assay) (*18, 37, 43*). As shown in Figure 3A, the concentration-dependence curves for human WT and its isolated N- and C-terminal domains (residues 1−189 and 190−243) demonstrate that the N-terminal domain is much less effective than WT apoA-I in solubilizing DMPC vesicles whereas the C-terminal domain is extremely effective (*18*). Interestingly, apoA-I h(1−189)/m(187−240) and h(1−220)/m(218−240) hybrid molecules displayed intermediate efficiencies between the human WT and the isolated human N-terminal domain despite the fact that the isolated mouse C-terminal domain (residues 187−240) itself was practically inactive. This suggests that the destabilized human N-terminal domain can interact with lipids effectively without the hydrophobic human C-terminal domain.

We also compared binding enthalpies of the human−mouse hybrid apoA-I to stable egg PC SUV (*11, 18*). As shown in Figure 3B, human WT and its isolated N- and C-terminal domains exhibited large exothermic heats whereas the mouse C-terminal domain exhibited almost no heat (*18*). However, both apoA-I h(1−189)/m(187−240) and h(1−220)/m(218−240) exhibited much larger exothermic heats compared to the human N-terminal domain, indicating that the destabilization of the human N-terminal domain promotes

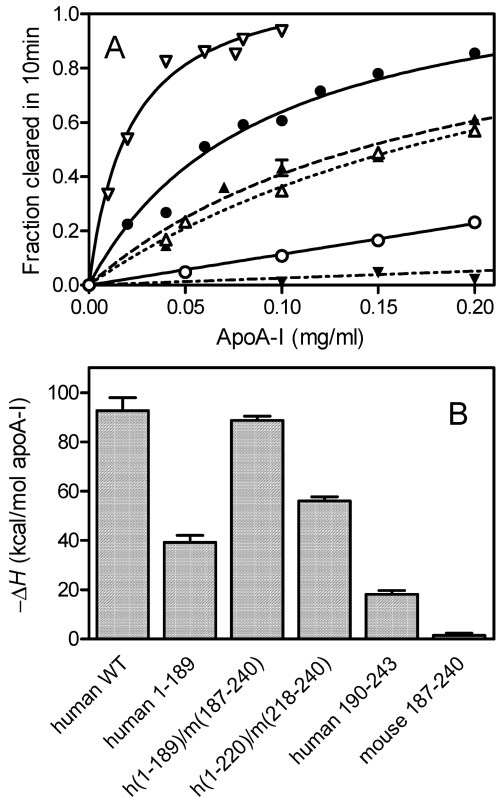

FIGURE 3: Solubilization of DMPC vesicles (A) and binding enthalpies to egg PC SUV (B) for human and mouse hybrid apoA-I. (A) Increases in fraction cleared of turbidity in 10 min after incubation of DMPC vesicles (0.25 mg/mL) with increasing concentration of protein at 24.6 °C are represented by ●, human WT; ○, human 1−189; ▲, apoA-I h(1−189)/m(187−240); △, apoA-I h(1−220)/m(218−240); ▽, human 190−243; and ▼, mouse 187−240. (B) Protein solutions were injected into excess SUV in an isothermal titration calorimeter at a PC-to-protein molar ratio of >10 000.

its lipid-binding capability by substituting the C-terminal α-helix with the equivalent mouse C-terminal segment. Consistent with this, much larger increases in α-helix content upon binding to SUV were observed in both h(1−189)/m(187−240) and h(1−220)/m(218−240) apoA-I (increases in α-helical amino acids are 69 and 62 residues, respectively) compared to the human 1−189 (26 residues).

Acrylodan Fluorescence. Next we employed site-specific labeling of apoA-I by acrylodan to probe the conformational properties and the spatial proximity of the N- and C-terminal domains in apoA-I. Acrylodan has been used for the site-specific conformational studies of proteins (*28, 29, 44, 45*) because it has several advantages as a fluorescence probe such as high sensitivity to the solvent environment and relatively low molecular weight. For attachment of acrylodan, we used two Cys-introduced mutants, V53C and F229C apoA-I. V53 and F229 are located in the putative N- and C-terminal α-helices (residues 44−65 and 220−241) of apoA-I, respectively, and our previous study revealed that neither the Cys mutagenesis nor the fluorescence labeling causes discernible changes in the lipid-free structure and lipid interaction of apoA-I (*46*).

Figure 4 shows the change in acrylodan emission spectra of apoA-I V53C−Ac when incubated at different concentrations of urea (from 0 to 6.4 M). Significant decreases in fluorescence intensity and red shifts in WMF of acrylodan were observed with increasing concentrations of urea,

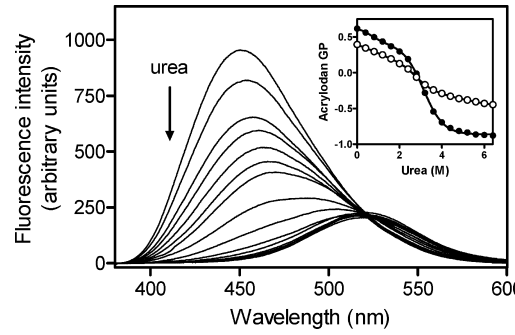

FIGURE 4: Acrylodan fluorescence emission spectra monitored at different concentrations of urea (from 0 to 6.4 M) for apoA-I V53C−Ac. The inset shows the change in acrylodan GP for apoA-I V53C−Ac (●) and F229C−Ac (○) as a function of urea concentration. Protein concentration was 25 μg/mL.

indicating transfer of the acrylodan molecule from the hydrophobic interior in a folded protein into an aqueous environment (*28, 45*). Such changes in spectroscopic properties of aminoacylnaphthalene derivatives have been described by GP, which is proportional to changes in the emission spectrum (*34, 47*). Since a decrease in GP value signifies an increase in the environment polarity of acrylodan, the difference in denaturation curves for apoA-I V53C−Ac and F229C−Ac monitored by acrylodan GP (Figure 4, inset) reflects the different stabilities of the N- and C-terminal helices in apoA-I against urea denaturation. As listed in Table 3, thermodynamic parameters of denaturation against GdnHCl and urea for apoA-I V53C−Ac and F229C−Ac indicate that V53 and F229 have similar stability against GdnHCl whereas V53 is more stable than F229 against urea. This suggests that both the N- and C-terminal helices have comparable conformational stability but that the N-terminal helix is stabilized more than the C-terminal helix via electrostatic interactions.

To further characterize the site-specific structure of the two domains, we compared WMF, fluorescence anisotropy, and KI quenching parameters of acrylodan fluorescence for apoA-I V53C−Ac and F229C−Ac (Table 4). The WMF values are 451 and 458 nm for V53C−Ac and F229C−Ac, respectively, indicating that both the N- and the C-terminal helices are in hydrophobic environments (*28*). Consistent with this, low K_{SV} values for both V53C−Ac and F229C−Ac suggest that both regions are shielded from the solvent. Interestingly, the acrylodan-labeled C-terminal helical peptide apoA-I 220−241/F229C−Ac exhibited a much higher WMF value corresponding to polarity in water (*28*) and a higher K_{SV} value compared to apoA-I F229C−Ac. In addition, fluorescence anisotropy reflecting the motional restriction of acrylodan was much lower in the peptide than in the apoA-I F229C−Ac. Taken together, these results suggest that the C-terminal helical region in the folded apoA-I molecule has a much more organized conformation than in the isolated helical peptide.

Finally, we measured the FRET from the Trp residues located in the N-terminal domain to acrylodan attached in the N- or C-terminal helices to confirm prior studies showing that the C-terminal segments are in close proximity to the N-terminal domain (*28, 29*). Compared to the unlabeled apoA-I V53C and F229C mutants, there were significant decreases in Trp emission fluorescence at around 335 nm and the concomitant appearance of an acrylodan fluorescence

Table 3: Parameters of Chemical Denaturation of apoA-I Variants Monitored by GP of Acrylodan Fluorescence

	GdnHCl denaturation			urea denaturation		
apoA-I variant	$\Delta G_D°$, kcal/mol	m	$D_{1/2}$, M	$\Delta G_D°$, kcal/mol	m	$D_{1/2}$, M
V53C−Ac	2.0 ± 0.1	1.5 ± 0.1	1.3 ± 0.1	2.6 ± 0.1	0.9 ± 0.1	2.9 ± 0.1
F229C−Ac	1.8 ± 0.1	1.3 ± 0.1	1.3 ± 0.1	1.5 ± 0.1	0.6 ± 0.1	2.5 ± 0.1

Table 4: WMF, Fluorescence Anisotropy, and KI Quenching Parameters of Acrylodan Fluorescence of apoA-I Variants and Peptide

			KI quenching	
apoA-I variant or peptide	WMF, nm[a]	fluorescence anisotropy	f_a	K_{SV}, M^{-1}
apoA-I V53C−Ac	451	0.152 ± 0.002	0.73 ± 0.05	3.1 ± 0.3
apoA-I F229C−Ac	460	0.140 ± 0.002	0.51 ± 0.04	3.7 ± 0.4
apoA-I 220−241/F229C−Ac	516	0.086 ± 0.004	0.60 ± 0.04	11.5 ± 0.6

[a] Estimated error is within ±3 nm.

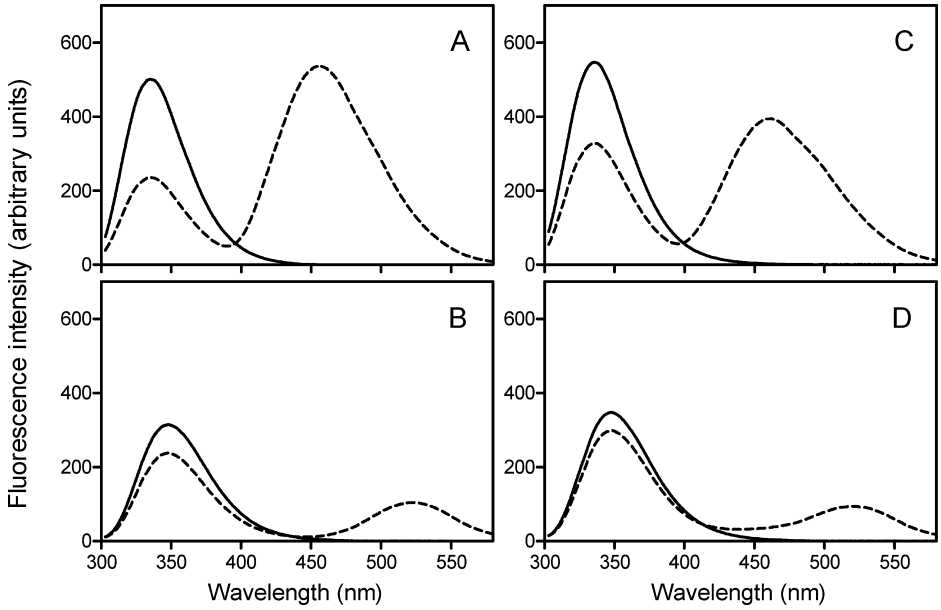

FIGURE 5: FRET between Trp residues in the N-terminal domain and acrylodan for apoA-I V53C−Ac (A and B) and F229C−Ac (C and D). Fluorescence emission spectra excited at 295 nm for unlabeled (solid lines) and acrylodan-labeled (dashed lines) apoA-I variants were recorded in the absence (A and C) or the presence (B and D) of 3 M GdnHCl. Protein concentration was 25 μg/mL.

peak at around 460 nm, indicating the occurrence of FRET from Trp residues to acrylodan in the folded apoA-I (Figure 5A,C). Because we monitored FRET at the protein concentration in which apoA-I exists completely as a monomer (*48*), the observed FRET dominantly comes from intramolecular interactions. The calculated FRET efficiency (E) and average distance (R) between the Trp residues and the acrylodan probe were 0.53 and 2.7 nm for apoA-I V53C−Ac and 0.40 and 2.9 nm for apoA-I F229C−Ac, respectively, indicating that the acrylodan probe attached at not only the N-terminal helix but also the C-terminal helix is in close proximity to Trp residues in the N-terminal domain. In contrast, after complete unfolding of apoA-I in the presence of 3 M GdnHCl, the difference in the Trp fluorescence between the unlabeled and the acrylodan-labeled apoA-I and acrylodan fluorescence peak became remarkably small (Figure 5B,D), indicating decreases in FRET due to increased separation of the Trp residues and acrylodan ($E = 0.24$ and 0.12 for apoA-I V53C−Ac and F229C−Ac, respectively). For apoA-I V53C−Ac, the proximity of the fluorophores in the primary sequence is likely to cause some FRET even in the presence of denaturant. A similar decrease in FRET for apoA-I F229C−Ac was also observed in the presence of 6 M urea (data not shown), suggesting that hydrophobic interaction contributes to the close proximity of the two domains.

DISCUSSION

The large exchangeable apolipoproteins such as apoA-I and apoE appear to share a common two-domain structure, in which the N-terminal, ~70%, of the molecule forms a helix bundle domain and the C-terminal domain exists as a discrete, less organized structure (*15, 19*). Recent studies using the C-terminal truncation variants indicated that this two-domain tertiary structure is also adopted by a new member of the exchangeable apolipoprotein family, apoA-V (*49, 50*). It is proposed that, in general, the N- and C-terminal elements in proteins have a tendency to be in contact, playing some special roles in protein folding and function (*51*). Indeed, it has been demonstrated that the C-terminal domain in apoE4 is in close contact with the N-terminal domain in the lipid-free state as well as on discoidal complexes because of the electrostatic interaction between the two domains (*52*). Recent cross-linking experiments for the lipid-bound conformation of apoA-I on discoidal complexes suggested that the N-terminal end folds back on itself, stabilizing an intermolecular interaction with the hydrophobic C-terminal

domain (*53*). Although the presence of the N- and C-terminal interaction in the lipid-free apoA-I molecule has also been proposed (*13, 14, 16, 25*), the experimental evidence has not been provided to date.

In our previous study comparing the structural stabilities of the N- and C-terminal domains in human and mouse apoA-I, near-UV CD measurements demonstrated that substitution of the C-terminal domain in human apoA-I by the mouse counterpart disorders the Trp packing in the N-terminal domain, whereas removal of the C-terminal domain from human apoA-I does not; this suggests that N- and C-terminal domain interactions affect the stability of the N-terminal helix bundle structure (*18*). The results of urea denaturation for the C-terminal truncated or substituted variants of human apoA-I (Figures 1 and 2 and Table 1) in this study clearly demonstrate that the C-terminal α-helical region (residues 223−243) is primarily responsible for the stabilization of the N-terminal helix bundle by the C-terminal domain. The finding that the disruption of the C-terminal α-helix by the proline insertion (L230P/L233P/Y236P) reduced the protein stability against urea denaturation (Figure 2) further indicates that the ability of this region to form α-helical structure is critical for the N- and C-terminal interaction. It should be noted that such stabilizing interactions between the N- and C-terminal domains are dominantly intramolecular because self-association of apoA-I does not occur under the condition in this study (*48*). Indeed, we did not detect any excimer fluorescence for the pyrene-labeled apoA-I in the C-terminal helical region (*46*), at least up to the concentration of 0.1 mg/mL (data not shown), indicating the absence of self-association through the C-terminal domain.

In apoE4, Arg-61 in the N-terminal domain forms a salt bridge with Glu-255 in the C-terminal domain (*54*), leading to the less organized and more exposed conformation of the C-terminal domain in apoE4 than occurs in apoE3 (*37, 55*). FRET and electron paramagnetic resonance measurements showed that such domain interaction in apoE4 results in a closer distance between the N- and the C-terminal domains than apoE3 (*52*). FRET analyses in the previous (*28, 29*) and the present (Figure 5) studies between Trp residues in the N-terminal domain and acrylodan attached in the C-terminal helix suggest that, like apoE4, the interaction between the N- and C-terminal domains in apoA-I causes the C-terminal α-helix to be in close proximity to the N-terminal helix bundle. Although these FRET data can be used to estimate only an average distance because of the presence of four Trp residues in the fluorescence energy donor, the derived average distance between Trp residues and F229C−acrylodan of 2.9 nm seems to be shorter than the calculated distances from the X-ray crystal structure of lipid-free apoA-I (2.6, 5.6, 3.5, and 3.1 nm from F229 to W8, W50, W72, and W108, respectively) (*17*). It is likely that such a close proximity of the two domains in the lipid-free apoA-I results in not only stabilization of the N-terminal helix bundle (Figures 1 and 2 and Table 1) but also the relatively less solvent-exposed, more organized conformation of the C-terminal helical region, which is comparable to the N-terminal helix bundle structure (Tables 3 and 4).

On the basis of the two-domain tertiary structure of apoA-I, we have proposed a two-step mechanism for the binding of apoA-I to a phospholipid surface (*15, 19*). In this model, the initial binding step occurs through hydrophobic amphipathic α-helices in the C-terminal domain (*26*), followed by a conformational opening of the N-terminal helix bundle to expose the hydrophobic faces of the amphipathic helices. In the first binding step, the C-terminal α-helix appears to separate from the N-terminal domain, perhaps converting helix−helix interactions between the two domains to lipid interactions of the C-terminal helix. This would result in the destabilization of the N-terminal helix bundle, which may trigger the conformational opening of the helix bundle in the second binding step. Interestingly, similar mechanisms by which the initial lipid interaction triggers the conformational opening of the helix bundle structure have been proposed for the lipid binding of apolipophorin III (*56*) and apoE (*57*).

Tertiary structural plasticity is thought to be functionally important for apolipoprotein binding to the lipid surface (*58, 59*). Indeed, the inverse correlation between the protein stability and the ability to transform phospholipid vesicles into discoidal complexes was observed for apolipoprotein III (*60, 61*) and the N-terminal domain of apoE isoforms (*43, 62*). In apoA-I, it was reported that deletion or mutation of both the N- and the C-terminal regions induces the less stable, molten globular-like conformation, possibly facilitating the protein binding to the lipid surface (*14, 32*). It was also demonstrated recently that, under acidic conditions, apoA-I increases its α-helical content and hydrophobicity, thereby promoting the formation of discoidal complexes (*63*). Consistent with these findings, we demonstrated in the present study that the destabilization of the human N-terminal domain by substituting the C-terminal domain or helical segment with the equivalent mouse counterparts promotes the lipid-binding ability of apoA-I (Figure 3). Thus, given the structural similarity of the N-terminal helix bundle among exchangeable apolipoproteins (*15, 19*), it is conceivable that besides the hydrophobicity and α-helix content of the C-terminal domain, the stability of the N-terminal helix bundle regulates the lipid-binding property of apoA-I (*18*). However, it should be noted that other reports showed that double deletion of the N- and C-terminal regions reduces or abolishes the lipid-binding ability of apoA-I despite the greatly reduced protein stability (*30, 31*).

Many plasma apolipoproteins such as apoA-I, apoA-II, apoC-II, and apoE display a high susceptibility to form or associate with amyloid fibrils both in vitro and in vivo (*64*), perhaps because of their partially folded, flexible conformation in the lipid-free state (*65*). Naturally occurring mutations in human apoA-I associated with hereditary amyloidosis are known to be all localized around the N-terminus of protein (*66*). Interestingly, in most cases of these mutated apoA-I, the N-terminal fragment is the predominant form of protein found in amyloid fibril deposits (*67*). Although the structural consequences of these mutations have not been defined yet, these findings suggest the possibility of an unstable N-terminal conformation being associated with mutations in this region. Since the C-terminal domain stabilizes the N-terminal helix bundle structure as shown in this study, it is tempting to speculate that the mutated apoA-I may be more susceptible to cleavage of the C-terminal domain, creating an unstable N-terminal fragment of apoA-I which may initiate the formation of amyloid fibrils (*68*).

In summary, this is the first characterization of the consequences for the N-terminal helix bundle domain of the interaction between the N- and the C-terminal tertiary structure domains that occurs in the apoA-I molecule. Our results demonstrated that the intramolecular domain−domain interaction in apoA-I causes the C-terminal α-helix to be in close proximity to the N-terminal helix bundle, modulating the conformational stability and functional properties of the helix bundle. Since the C-terminal α-helical segment is responsible for this stabilizing interaction between the two domains, the C-terminal domain appears to play a role in lipid binding of apoA-I not only through its hydrophobic α-helical structure but also by triggering the conformational change of the N-terminal helix bundle. In addition, the apoA-I mutations associated with hereditary amyloidosis may alter the domain interaction, resulting in an unstable, partially folded conformation of the N-terminal helix bundle which appears to be a crucial characteristic for the formation of amyloid fibrils.

ACKNOWLEDGMENT

The authors thank Drs. Saburo Aimoto and Toru Kawakami (Institute for Protein Research, Osaka University, Japan) for their help with ITC measurements.

REFERENCES

1. Curtiss, L. K., Valenta, D. T., Hime, N. J., and Rye, K. A. (2006) What is so special about apolipoprotein AI in reverse cholesterol transport? *Arterioscler., Thromb., Vasc. Biol. 26*, 12–19.
2. Rader, D. J. (2006) Molecular regulation of HDL metabolism and function: implications for novel therapies. *J. Clin. Invest. 116*, 3090–3100.
3. Tall, A. R., Yvan-Charvet, L., Terasaka, N., Pagler, T., and Wang, N. (2008) HDL, ABC transporters, and cholesterol efflux: implications for the treatment of atherosclerosis. *Cell Metab. 7*, 365–375.
4. Krimbou, L., Marcil, M., and Genest, J. (2006) New insights into the biogenesis of human high-density lipoproteins. *Curr. Opin. Lipidol. 17*, 258–267.
5. Oram, J. F., and Vaughan, A. M. (2006) ATP-Binding cassette cholesterol transporters and cardiovascular disease. *Circ. Res. 99*, 1031–1043.
6. Chroni, A., Liu, T., Fitzgerald, M. L., Freeman, M. W., and Zannis, V. I. (2004) Cross-linking and lipid efflux properties of apoA-I mutants suggest direct association between apoA-I helices and ABCA1. *Biochemistry 43*, 2126–2139.
7. Vedhachalam, C., Duong, P. T., Nickel, M., Nguyen, D., Dhanasekaran, P., Saito, H., Rothblat, G. H., Lund-Katz, S., and Phillips, M. C. (2007) Mechanism of ATP-binding cassette transporter A1-mediated cellular lipid efflux to apolipoprotein A-I and formation of high density lipoprotein particles. *J. Biol. Chem. 282*, 25123–25130.
8. Hassan, H. H., Denis, M., Lee, D. Y., Iatan, I., Nyholt, D., Ruel, I., Krimbou, L., and Genest, J. (2007) Identification of an ABCA1-dependent phospholipid-rich plasma membrane apolipoprotein A-I binding site for nascent HDL formation: implications for current models of HDL biogenesis. *J. Lipid Res. 48*, 2428–2442.
9. Segrest, J. P., Jones, M. K., De Loof, H., Brouillette, C. G., Venkatachalapathi, Y. V., and Anantharamaiah, G. M. (1992) The amphipathic helix in the exchangeable apolipoproteins: a review of secondary structure and function. *J. Lipid Res. 33*, 141–166.
10. Palgunachari, M. N., Mishra, V. K., Lund-Katz, S., Phillips, M. C., Adeyeye, S. O., Alluri, S., Anantharamaiah, G. M., and Segrest, J. P. (1996) Only the two end helixes of eight tandem amphipathic helical domains of human apo A-I have significant lipid affinity. Implications for HDL assembly. *Arterioscler., Thromb., Vasc. Biol. 16*, 328–338.
11. Saito, H., Dhanasekaran, P., Nguyen, D., Deridder, E., Holvoet, P., Lund-Katz, S., and Phillips, M. C. (2004) α-Helix formation is required for high affinity binding of human apolipoprotein A-I to lipids. *J. Biol. Chem. 279*, 20974–20981.
12. Wang, L., Hua, N., Atkinson, D., and Small, D. M. (2007) The N-terminal (1−44) and C-terminal (198−243) peptides of apolipoprotein A-I behave differently at the triolein/water interface. *Biochemistry 46*, 12140–12151.
13. Fang, Y., Gursky, O., and Atkinson, D. (2003) Structural studies of N- and C-terminally truncated human apolipoprotein A-I. *Biochemistry 42*, 6881–6890.
14. Tanaka, M., Dhanasekaran, P., Nguyen, D., Ohta, S., Lund-Katz, S., Phillips, M. C., and Saito, H. (2006) Contributions of the N- and C-terminal helical segments to the lipid-free structure and lipid interaction of apolipoprotein A-I. *Biochemistry 45*, 10351–10358.
15. Saito, H., Dhanasekaran, P., Nguyen, D., Holvoet, P., Lund-Katz, S., and Phillips, M. C. (2003) Domain structure and lipid interaction in human apolipoproteins A-I and E, a general model. *J. Biol. Chem. 278*, 23227–23232.
16. Silva, R. A., Hilliard, G. M., Fang, J., Macha, S., and Davidson, W. S. (2005) A three-dimensional molecular model of lipid-free apolipoprotein A-I determined by cross-linking/mass spectrometry and sequence threading. *Biochemistry 44*, 2759–2769.
17. Ajees, A. A., Anantharamaiah, G. M., Mishra, V. K., Hussain, M. M., and Murthy, H. M. (2006) Crystal structure of human apolipoprotein A-I: insights into its protective effect against cardiovascular diseases. *Proc. Natl. Acad. Sci. U.S.A. 103*, 2126–2131.
18. Tanaka, M., Koyama, M., Dhanasekaran, P., Nguyen, D., Nickel, M., Lund-Katz, S., Saito, H., and Phillips, M. C. (2008) Influence of tertiary structure domain properties on the functionality of apolipoprotein A-I. *Biochemistry 47*, 2172–2180.
19. Saito, H., Lund-Katz, S., and Phillips, M. C. (2004) Contributions of domain structure and lipid interaction to the functionality of exchangeable human apolipoproteins. *Prog. Lipid Res. 43*, 350–380.
20. Reschly, E. J., Sorci-Thomas, M. G., Davidson, W. S., Meredith, S. C., Reardon, C. A., and Getz, G. S. (2002) Apolipoprotein A-I alpha-helices 7 and 8 modulate high density lipoprotein subclass distribution. *J. Biol. Chem. 277*, 9645–9654.
21. Rubin, E. M., Ishida, B. Y., Clift, S. M., and Krauss, R. M. (1991) Expression of human apolipoprotein A-I in transgenic mice results in reduced plasma levels of murine apolipoprotein A-I and the appearance of two new high density lipoprotein size subclasses. *Proc. Natl. Acad. Sci. U.S.A. 88*, 434–438.
22. Davidson, W. S., and Thompson, T. B. (2007) The structure of apolipoprotein A-I in high density lipoproteins. *J. Biol. Chem. 282*, 22249–22253.
23. Thomas, M. J., Bhat, S., and Sorci-Thomas, M. G. (2008) Three dimensional models of high density lipoprotein apoA-I: Implications for its assembly and function. *J. Lipid Res. 49*, 1875–1883.
24. Davidson, W. S., Hazlett, T., Mantulin, W. W., and Jonas, A. (1996) The role of apolipoprotein AI domains in lipid binding. *Proc. Natl. Acad. Sci. U.S.A. 93*, 13605–13610.
25. Lagerstedt, J. O., Budamagunta, M. S., Oda, M. N., and Voss, J. C. (2007) Electron paramagnetic resonance spectroscopy of site-directed spin labels reveals the structural heterogeneity in the N-terminal domain of apoA-I in solution. *J. Biol. Chem. 282*, 9143–9149.
26. Oda, M. N., Forte, T. M., Ryan, R. O., and Voss, J. C. (2003) The C-terminal domain of apolipoprotein A-I contains a lipid-sensitive conformational trigger. *Nat. Struct. Biol. 10*, 455–460.
27. Gross, E., Peng, D. Q., Hazen, S. L., and Smith, J. D. (2006) A novel folding intermediate state for apolipoprotein A-I: role of the amino and carboxy termini. *Biophys. J. 90*, 1362–1370.
28. Tricerri, M. A., Behling Agree, A. K., Sanchez, S. A., and Jonas, A. (2000) Characterization of apolipoprotein A-I structure using a cysteine-specific fluorescence probe. *Biochemistry 39*, 14682–14691.
29. Behling Agree, A. K., Tricerri, M. A., Arnvig McGuire, K., Tian, S. M., and Jonas, A. (2002) Folding and stability of the C-terminal half of apolipoprotein A-I examined with a Cys-specific fluorescence probe. *Biochim. Biophys. Acta 1594*, 286–296.
30. Fang, Y., Gursky, O., and Atkinson, D. (2003) Lipid-binding studies of human apolipoprotein A-I and its terminally truncated mutants. *Biochemistry 42*, 13260–13268.
31. Chroni, A., Liu, T., Gorshkova, I., Kan, H. Y., Uehara, Y., Von Eckardstein, A., and Zannis, V. I. (2003) The central helices of ApoA-I can promote ATP-binding cassette transporter A1 (ABCA1)-mediated lipid efflux. Amino acid residues 220−231 of the wild-type ApoA-I are required for lipid efflux in vitro and high density lipoprotein formation in vivo. *J. Biol. Chem. 278*, 6719–6730.

32. Beckstead, J. A., Block, B. L., Bielicki, J. K., Kay, C. M., Oda, M. N., and Ryan, R. O. (2005) Combined N- and C-terminal truncation of human apolipoprotein A-I yields a folded, functional central domain. *Biochemistry 44*, 4591–4599.
33. Sparks, D. L., Lund-Katz, S., and Phillips, M. C. (1992) The charge and structural stability of apolipoprotein A-I in discoidal and spherical recombinant high density lipoprotein particles. *J. Biol. Chem. 267*, 25839–25847.
34. Parasassi, T., De Stasio, G., Ravagnan, G., Rusch, R. M., and Gratton, E. (1991) Quantitation of lipid phases in phospholipid vesicles by the generalized polarization of Laurdan fluorescence. *Biophys. J. 60*, 179–189.
35. Saito, H., Minamida, T., Arimoto, I., Handa, T., and Miyajima, K. (1996) Physical states of surface and core lipids in lipid emulsions and apolipoprotein binding to the emulsion surface. *J. Biol. Chem. 271*, 15515–15520.
36. Flora, K., Brennan, J. D., Baker, G. A., Doody, M. A., and Bright, F. V. (1998) Unfolding of acrylodan-labeled human serum albumin probed by steady-state and time-resolved fluorescence methods. *Biophys. J. 75*, 1084–1096.
37. Sakamoto, T., Tanaka, M., Vedhachalam, C., Nickel, M., Nguyen, D., Dhanasekaran, P., Phillips, M. C., Lund-Katz, S., and Saito, H. (2008) Contributions of the carboxyl-terminal helical segment to the self-association and lipoprotein preferences of human apolipoprotein E3 and E4 isoforms. *Biochemistry 47*, 2968–2977.
38. Saito, H., Dhanasekaran, P., Baldwin, F., Weisgraber, K. H., Lund-Katz, S., and Phillips, M. C. (2001) Lipid binding-induced conformational change in human apolipoprotein E. Evidence for two lipid-bound states on spherical particles. *J. Biol. Chem. 276*, 40949–40954.
39. Brouillette, C. G., Anantharamaiah, G. M., Engler, J. A., and Borhani, D. W. (2001) Structural models of human apolipoprotein A-I: a critical analysis and review. *Biochim. Biophys. Acta 1531*, 4–46.
40. Monera, O. D., Kay, C. M., and Hodges, R. S. (1994) Protein denaturation with guanidine hydrochloride or urea provides a different estimate of stability depending on the contributions of electrostatic interactions. *Protein Sci. 3*, 1984–1991.
41. Ramsay, G., Ionescu, R., and Eftink, M. R. (1995) Modified spectrophotometer for multi-dimensional circular dichroism/ fluorescence data acquisition in titration experiments: application to the pH and guanidine-HCI induced unfolding of apomyoglobin. *Biophys. J. 69*, 701–707.
42. Vedhachalam, C., Liu, L., Nickel, M., Dhanasekaran, P., Anantharamaiah, G. M., Lund-Katz, S., Rothblat, G. H., and Phillips, M. C. (2004) Influence of ApoA-I structure on the ABCA1-mediated efflux of cellular lipids. *J. Biol. Chem. 279*, 49931–49939.
43. Segall, M. L., Dhanasekaran, P., Baldwin, F., Anantharamaiah, G. M., Weisgraber, K. H., Phillips, M. C., and Lund-Katz, S. (2002) Influence of apoE domain structure and polymorphism on the kinetics of phospholipid vesicle solubilization. *J. Lipid Res. 43*, 1688–1700.
44. Krishnan, R., and Lindquist, S. L. (2005) Structural insights into a yeast prion illuminate nucleation and strain diversity. *Nature 435*, 765–772.
45. Sun, Y., Breydo, L., Makarava, N., Yang, Q., Bocharova, O. V., and Baskakov, I. V. (2007) Site-specific conformational studies of prion protein (PrP) amyloid fibrils revealed two cooperative folding domains within amyloid structure. *J. Biol. Chem. 282*, 9090–9097.
46. Kono, M., Okumura, Y., Tanaka, M., Nguyen, D., Dhanasekaran, P., Lund-Katz, S., Phillips, M. C., and Saito, H. (2008) Conformational flexibility of the N-terminal domain of apolipoprotein a-I bound to spherical lipid particles. *Biochemistry 47*, 11340–11347.
47. Krasnowska, E. K., Gratton, E., and Parasassi, T. (1998) Prodan as a membrane surface fluorescence probe: partitioning between water and phospholipid phases. *Biophys. J. 74*, 1984–1993.
48. Davidson, W. S., Arnvig-McGuire, K., Kennedy, A., Kosman, J., Hazlett, T. L., and Jonas, A. (1999) Structural organization of the N-terminal domain of apolipoprotein A-I: studies of tryptophan mutants. *Biochemistry 38*, 14387–14395.
49. Beckstead, J. A., Wong, K., Gupta, V., Wan, C. P., Cook, V. R., Weinberg, R. B., Weers, P. M., and Ryan, R. O. (2007) The C terminus of apolipoprotein A-V modulates lipid-binding activity. *J. Biol. Chem. 282*, 15484–15489.
50. Wong, K., Beckstead, J. A., Lee, D., Weers, P. M., Guigard, E., Kay, C. M., and Ryan, R. O. (2008) The N-terminus of apolipoprotein A-V adopts a helix bundle molecular architecture. *Biochemistry 47*, 8768–8774.
51. Krishna, M. M., and Englander, S. W. (2005) The N-terminal to C-terminal motif in protein folding and function. *Proc. Natl. Acad. Sci. U.S.A. 102*, 1053–1058.
52. Hatters, D. M., Budamagunta, M. S., Voss, J. C., and Weisgraber, K. H. (2005) Modulation of apolipoprotein E structure by domain interaction: differences in lipid-bound and lipid-free forms. *J. Biol. Chem. 280*, 34288–34295.
53. Bhat, S., Sorci-Thomas, M. G., Alexander, E. T., Samuel, M. P., and Thomas, M. J. (2005) Intermolecular contact between globular N-terminal fold and C-terminal domain of ApoA-I stabilizes its lipid-bound conformation: studies employing chemical cross-linking and mass spectrometry. *J. Biol. Chem. 280*, 33015–33025.
54. Dong, L. M., and Weisgraber, K. H. (1996) Human apolipoprotein E4 domain interaction. Arginine 61 and glutamic acid 255 interact to direct the preference for very low density lipoproteins. *J. Biol. Chem. 271*, 19053–19057.
55. Saito, H., Dhanasekaran, P., Baldwin, F., Weisgraber, K. H., Phillips, M. C., and Lund-Katz, S. (2003) Effects of polymorphism on the lipid interaction of human apolipoprotein E. *J. Biol. Chem. 278*, 40723–40729.
56. Narayanaswami, V., Wang, J., Schieve, D., Kay, C. M., and Ryan, R. O. (1999) A molecular trigger of lipid binding-induced opening of a helix bundle exchangeable apolipoprotein. *Proc. Natl. Acad. Sci. U.S.A. 96*, 4366–4371.
57. Lu, B., Morrow, J. A., and Weisgraber, K. H. (2000) Conformational reorganization of the four-helix bundle of human apolipoprotein E in binding to phospholipid. *J. Biol. Chem. 275*, 20775–20781.
58. Morrow, J. A., Hatters, D. M., Lu, B., Hochtl, P., Oberg, K. A., Rupp, B., and Weisgraber, K. H. (2002) Apolipoprotein E4 forms a molten globule. A potential basis for its association with disease. *J. Biol. Chem. 277*, 50380–50385.
59. Guha, M., Gao, X., Jayaraman, S., and Gursky, O. (2008) Correlation of structural stability with functional remodeling of high-density lipoproteins: the importance of being disordered. *Biochemistry 47*, 11393–11397.
60. Weers, P. M., Kay, C. M., and Ryan, R. O. (2001) Conformational changes of an exchangeable apolipoprotein, apolipophorin III from Locusta migratoria, at low pH: correlation with lipid binding. *Biochemistry 40*, 7754–7760.
61. Weers, P. M., Abdullahi, W. E., Cabrera, J. M., and Hsu, T. C. (2005) Role of buried polar residues in helix bundle stability and lipid binding of apolipophorin III: destabilization by threonine 31. *Biochemistry 44*, 8810–8816.
62. Weers, P. M., Narayanaswami, V., Choy, N., Luty, R., Hicks, L., Kay, C. M., and Ryan, R. O. (2003) Lipid binding ability of human apolipoprotein E N-terminal domain isoforms: correlation with protein stability? *Biophys. Chem. 100*, 481–492.
63. Fukuda, M., Nakano, M., Miyazaki, M., Tanaka, M., Saito, H., Kobayashi, S., Ueno, M., and Handa, T. (2008) Conformational change of apolipoprotein A-I and HDL formation from model membranes under intracellular acidic conditions. *J. Lipid Res. 49*, 2419–2426.
64. Hatters, D. M., and Howlett, G. J. (2002) The structural basis for amyloid formation by plasma apolipoproteins: a review. *Eur. Biophys. J. 31*, 2–8.
65. Uversky, V. N., and Fink, A. L. (2004) Conformational constraints for amyloid fibrillation: the importance of being unfolded. *Biochim. Biophys. Acta 1698*, 131–153.
66. Sorci-Thomas, M. G., and Thomas, M. J. (2002) The effects of altered apolipoprotein A-I structure on plasma HDL concentration. *Trends Cardiovasc. Med. 12*, 121–128.
67. Genschel, J., Haas, R., Propsting, M. J., and Schmidt, H. H. (1998) Apolipoprotein A-I induced amyloidosis. *FEBS Lett. 430*, 145–149.
68. Liz, M. A., Gomes, C. M., Saraiva, M. J., and Sousa, M. M. (2007) ApoA-I cleaved by transthyretin has reduced ability to promote cholesterol efflux and increased amyloidogenicity. *J. Lipid Res. 48*, 2385–2395.

BI802317V